AGRICULTURAL TYRE STIFFNESS CHANGE AS A FUNCTION OF TYRE WEAR

Carl Becker[a] and Schalk Els[a]

[a] *University of Pretoria, 1 Lynnwood Road, Pretoria, 0002, SOUTH AFRICA*

carl.becker@up.ac.za, schalk.els@up.ac.za

Vehicle designers use tyre characteristic parameters to parameterize tyre models during the design phase of a vehicle to determine the ride comfort, handling and performance. Tyre data is mostly presented only for new tyres with 100% tread on them. Soft terrain traction and minimal compaction have always been major requirements for agricultural tyres, however agricultural vehicles are increasingly being used on asphalt/non-deformable terrain as commercial farms are ever increasing in size. As operational costs are always forced to a minimum, agricultural vehicles operate with tyres ranging from new to fully used condition ranging from 100% down to almost 0% tread on them. During the operational life of a tyre the tyre characteristics change as the tyre tread wears down. This study investigates the change in tyre characteristics on hard terrain with tyre wear at a single load condition, two different inflation pressures and three tread wear conditions. Significant trends are noted with dramatic changes in traction and tyre stiffnesses as the tyre wear changes.

Keywords: agricultural tyre, tyre wear, P80 sandpaper, longitudinal stiffness, lateral stiffness, vertical stiffness, cleat, inflation pressure, tyre characteristics

1. Introduction

Agricultural vehicles are increasingly being used on asphalt/non-deformable terrain as commercial farms are ever increasing in size. Thus, farmers need to travel with agricultural vehicles over long distances on public roads from one field to the next. This drives the operating conditions of

these vehicles to the limit. As operational costs are always forced to a minimum, agricultural vehicles operate with tyres ranging from new to fully used condition ranging from 100% down to almost 0% tread on them. During the operational life of a tyre the tyre characteristics change as the tyre wears. This is not always taken into consideration by the Original Equipment Manufacturers (OEMs), as it is expected from the end user to conduct the required maintenance on the vehicle. New tread designs on tyres are also increasing the forces on the drivetrain as the tyres designed for on-road use for agricultural vehicles have a larger footprint with more rubber in contact with the road.

Every wheeled vehicle used on earth or any other planet is exposed to tyre wear. Tyres are available in an endless variety of sizes, load ratings, tread patterns and material compounds. Tyres are the only components in the wheeled-vehicle system that connects the vehicle with the terrain over which the vehicle travels. This can range from a single wheel up to multiple wheels, depending on the vehicle and application.

Tyres can be manufactured from multiple materials ranging from metals to rubber. Over the last decade considerable advances have been made in the levels of detail design and simulation of large off-road vehicles used in construction, mining and agricultural industries amongst others. These advances in simulation have been driven as many of these large vehicles, which still fit within the legal road limits, are being used on public roads and thus they need to comply with stricter national road traffic regulations all over the world.

Even with the larger vehicles the OEMs have to compete with increased production requirements on the one hand, which means faster operating conditions and on the other hand stricter industrial regulations, emissions regulations, road safety regulations as well as Occupational Health and Safety (OHS) regulations. Virtual test rigs have become more important in the development process of all vehicles (Dressler et al, 2009). This has forced OEMs to invest in more detailed simulation orientated design processes to increase safety and efficiency of the vehicles. The increase in production

operating conditions typically drives improved handling characteristics and lower operating costs as the vehicles need to travel safely at higher speeds over longer distances.

The tyres play a very important role in all of these considerations. Obtaining tyre data is not a trivial or inexpensive exercise, as a result tyre manufactures are reluctant to freely supply tyre data and only supply high-end clients with limited tyre data. Test equipment suitable for large agricultural and off-road vehicles are very limited. Vehicle OEMs use tyre characteristics parameters during the design phase of a vehicle to determine the required design safety factors to be used in the driveline as well as to evaluate the ride comfort, handling and performance of the vehicles. These parameters are most of the time only available for new tyres with 100% tread on them.

A number of studies were conducted in the 1970's to the 1990's to obtain tyre data. Crolla and Maclaurin (1985) already described the importance and contribution that simulation makes in the design stage. Limited information regarding the suspension characteristics of agricultural tyres are available as described by Stayner et al. (1984) and poor information about the tyre's behavior over any terrain has a significant effect on the simulation errors (Lines 1991). Wright et.al, (2019) indicated that tyre wear and aging does not have a significant change in Sports Utility Vehicle's (SUV) tyre characteristics, however the tread depth on SUV tyres are of order of the carcass thickness compared to agricultural and construction tyres where the tread thickness can be up to 10 times the carcass thickness. The thick tread blocks on these large tyres make a significant contribution to the stiffness and mass of the tyre, thus as the tread wears down the tyre characteristics changes.

Simulation results are only as reliable as the input data and in vehicle ride or handling simulations the primary excitation into the vehicle is via the tyres, thus the importance of having reliable tyre data for accurate tyre modeling and vehicle simulation. With the tyres being the only suspension on many agricultural and construction vehicles, the importance of accurate tyre models is even more critical. The advances made in tyre technology to date have placed a large question mark on the reliability on the limited historical collection of tyre data available especially in the agricultural and construction

industry. Other vehicle factors that are affected by the tyre characteristics range from off-road traction and soil compaction to on-road handling, ride comfort, braking and motion resistance.

This paper investigates the change in tyre characteristics with tyre tread wear at a single load condition, two different inflation pressures and three tread wear conditions. Interesting results are noted with a dramatic change in traction and tyre stiffnesses as the tyre tread depth changes.

2. Measuring Tyre Characteristics

Literature has indicated very little new research on agricultural tyres (this may be the case for literature published in English), although tyre manufacturers are constantly changing the carcass designs and improving the durability of agricultural and construction tyre. Only a limited number of test rigs for large diameter tyres are available across the world, which limits the amount of research conducted on large diameter tyres. Tyre characteristics can be measured by multiple methods. Each method has different constraints and has its own advantages and drawbacks. This is the case for passenger cars, motorsport, motorcycle, commercial truck, heavy duty trucks, agricultural and construction vehicles. Many test laboratories are spread worldwide and most have the capability to parameterize relatively small tyres (truck tyres up to 50kN vertical load, (fka, 2021)). Larger tyres present challenges as large amounts of driving power and infrastructure are required to test these tyres at the designed loads. Only a few examples of test equipment are referenced in this paper. Typical indoor laboratory test rigs are drum test rigs or flat track rigs. Some test rigs can only be used for traction characterization, where other test rigs can conduct side force vs. slip angle tests, rolling resistance measurements or even simulate track racing conditions. MTS (2021) is one of the large supplier of tyre test rigs.

The University of Hohenheim has multiple large tyre test rigs in the form of a flat belt test stand, single wheel test trailer and an instrumented test tractor (Witzel, 2018). These test rigs can be used to measure longitudinal forces, lateral forces and rolling resistance on larger agricultural tyres. Other single wheel test trailers have been built for agricultural tyres, used and upgraded since the early 1960's. These trailers can be used on any terrain. Billington (1973) introduced the NIAE MkII single wheel tester in 1973. Crolla and El-Razaz (1987) presented some results measured on deformable terrain. Ambruster and Kutzbach (1989), developed a single wheel tester which tests a driven wheel at pre-set slip angles. Shmuleviuch et al. (1996) presented a new field single wheel tester. It is unknown if all these single wheel testers are still in service. Currently the University of Hohenheim's single wheel tester can test tyres with diameters up to 2000 mm at vertical loads up to 40 kN, (Witzel, 2018). Mardani et al. (2010) from the Faculty of Agriculture at the Urmia University, Iran, uses a single wheel tester in a soil bin to determine the motion resistance and traction with variation in dynamic loading, ballasting, travel speeds and tyre inflation pressures.

Previous studies by Misiewicz et al. (2016) compared methods for estimating the carcass stiffness of agricultural tyres (600/55-26.5 implement tyre) on hard surfaces indicated that the tread on an agricultural tyre has an effect on the vertical deflection, however it has no effect on the slope of the load vs. deflection characteristics. This study further investigated the contact pressure change for different tyre inflation pressures on a treaded and smooth tyre. It was concluded that the tyre vertical load and inflation pressure have a significant effect on the mean and maximum surface contact pressure on a smooth tyre compared to a treaded tyre where only the inflation pressure had an influence on the resulting contact pressure. These findings agreed with studies by Karafiath and Nowatzki (1978). Misiewicz et al. (2016) concluded that the carcass stiffness of the treaded implement tyre was significantly greater compared to the carcass stiffness of the smooth tyre. Misiewicz (2010) observed that tyres maintain a near constant contact area when the tyres are loaded

with the recommended inflation pressure as specified by the tyre manufacture. This is expected and the reason why tyre manufacturers supply the user with recommended inflation pressures for specific load applications. Murphy and Lines (1991) conducted a comprehensive study on the stiffness of agricultural tractor tyres and found the inflation pressure, rolling speed, tyre size and tyre age have the largest effect on the vertical stiffness where the tyre lug length and the type of surface does have some influence. Murphy and Lines (1991) also proposed the vertical stiffness to be estimated from the tyre size, inflation pressure and age using eq. (1)

$$K_t = 172 - 1.77D + 5.6A + 0.34WDP \qquad \text{eq. (1)}$$

where K_t is the stiffness (kN/m), W and D are the tyre section width and rim diameter, respectively, in inches. A is the tyre age in years with P the inflation pressure in bar.

The Vehicle Dynamics Group (VDG) at the Department of Mechanical and Aeronautical Engineering of the University of Pretoria in South Africa, has developed a Dynamic Tyre Test Trailer (DTTT) and a Static Tyre Test Rig (STTR) as presented by Becker and Els (2018). The DTTT tests two of the same tyres simultaneously in opposed lateral slip directions at a maximum load of 50kN per wheel. The DTTT can measure tyre forces and moments with the use of wheel force transducers during lateral force vs. slip angle measurements, longitudinal force vs. longitudinal slip measurements as well as combined lateral and longitudinal force measurements during braking at pre-determined lateral slip angles. The DTTT is shown in Figure 1. The STTR can measure the static stiffness of a tyre in the longitudinal or lateral direction for a predetermined vertical load. The STTR is equipped with 1MN actuators and can accommodate tyres from 800mm to 4000mm diameter. The STTR is shown in Figure 2. The STTR was used during this study to investigate the change in tyre characteristics due to tyre tread wear on the tyre in question. Limited assessments on the longitudinal/

tractional stiffness and lateral stiffnesses were conducted in previous studies at different tyre wear conditions (Misiewicz et al, 2016). These stiffnesses are the important factors when considering the loads on the driveline and handling characteristics of the vehicles and are therefore included in this study.

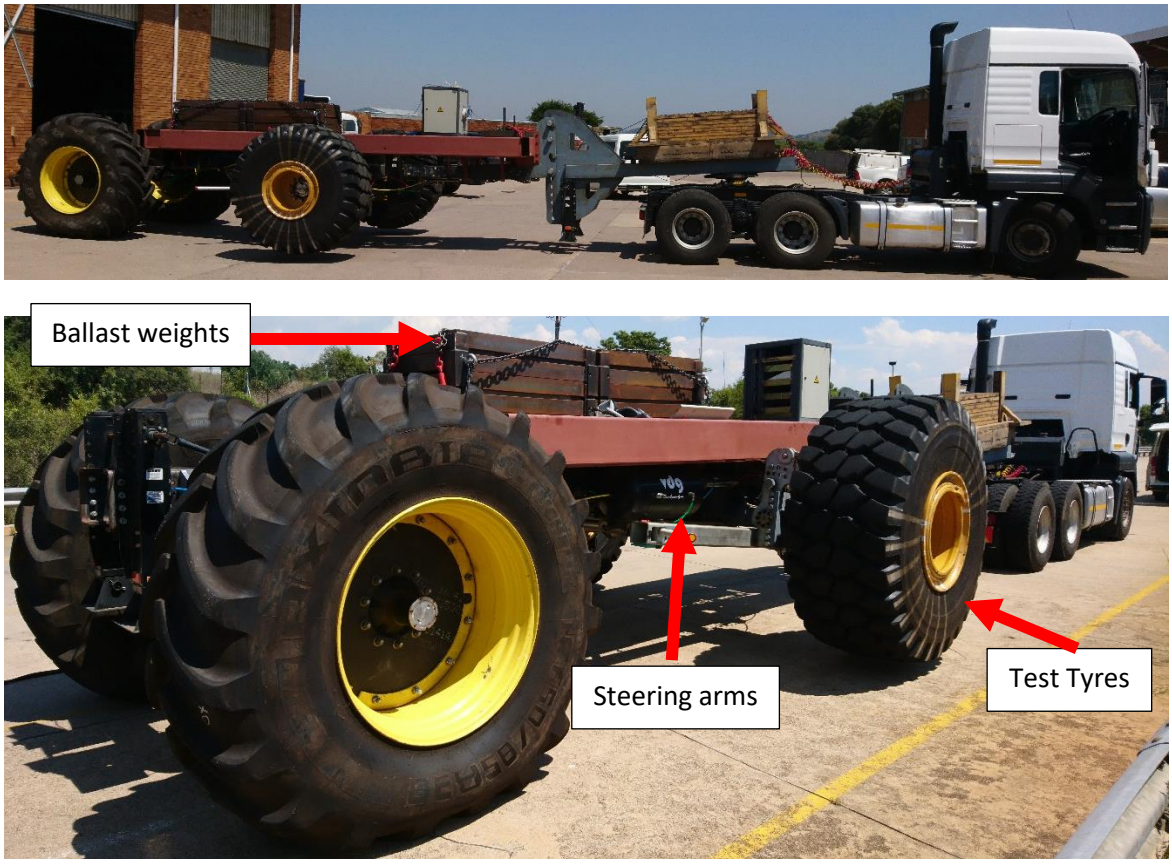

Figure 1: Dynamic Tyre Test Trailer from the Vehicle Dynamics Group at the University of Pretoria.

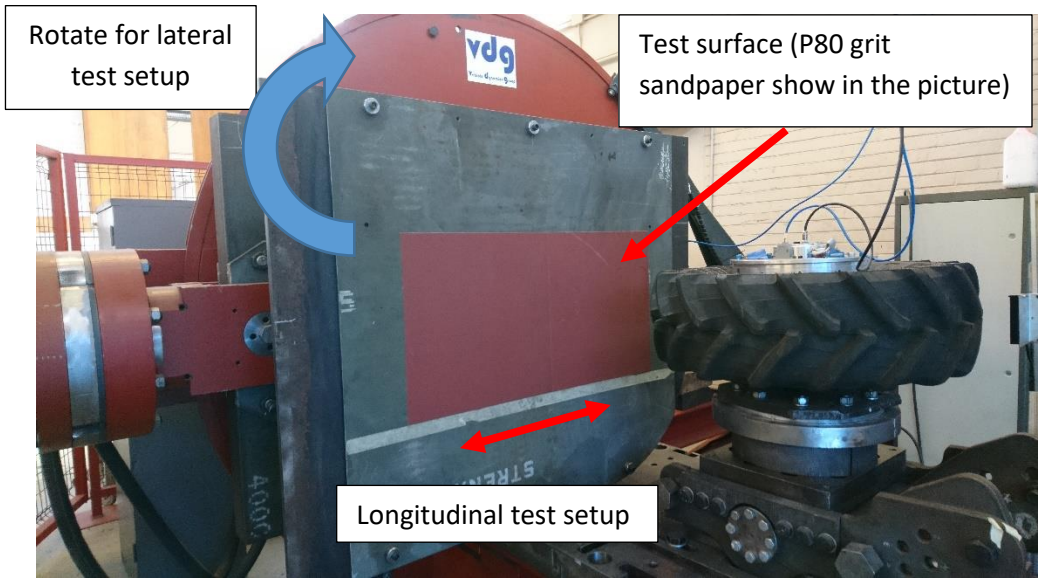

Figure 2: Static Tyre Test Rig from the Vehicle Dynamics Group at the University of Pretoria: Longitudinal test setup.

3. Measuring the Change in Tyre Characteristics as a Function of Tyre Wear

Measuring tyre characteristics on any tyre is not a trivial exercise. The logistics, setup time and costs increase dramatically with tyre size. The following section describes the tyre and the equipment used during this study.

3.1 Tyre of Interest

The tyre of interest for this study is a Trelleborg TM700-280/70R16 agricultural large lug tyre with a load index of 112 (1120kg) and speed rating of A8 (40km/h). This tyre was previously used to compare methods for measuring motion resistance (Becker and Els, 2020).

In this study the tyre characteristics in the form of longitudinal, lateral and vertical stiffness of the tyre at two inflation pressures for 100% tread, 50% tread and 0% tread were determined for a single load case of 5.68kN. A single load case was selected to be able to investigate the effect the tread wear on a tyre will have during the life of the tyre when mounted on a vehicle. Figure 3 shows the condition

of the tyres used during this study. The mass of the tyre as mounted on the rim for the different tread wear conditions are noted in Table 1. The change in tyre mass due to the tread wear is significant and the tyre loses 7.5kg or 31% of its mass. The different tread conditions were as follows:

- 100% Tread – New tyre, run-in, static tests conducted post motion resistance tests, (Becker and Els, 2020), where no traction or braking was applied to the tyre. Tread depth at 30mm.
- 50% Tread – 15mm of tread shaved with tyre regrooving tool with surface buffed post shaving.
- 0% Tread – Additional 15mm of tread shaved and tyre buffed post shaving.

a) *b)*

Figure 3: a)Trelleborg TM700-280/70R16 tyre with 100% tread, b)Trelleborg TM700-280/70R16 tyre with 50% and 0% tread respectively.

Table 1: Mass of test tyre for different tread wear conditions.

Tread wear condition	Tyre mass [kg]	% Change in tyre mass
100% Tread	24	-
50% Tread	22	8%
0% Tread	16.5	31%

3.2 Static Stiffness Tests

Static stiffness tests were conducted to measure the vertical, longitudinal and lateral stiffness at two inflation pressures of 80kPa and 200kPa using the STTR as shown in Figure 2. The inflation pressures and vertical load at which the longitudinal and lateral stiffness were measured, were selected from the tyre manufacturer data sheet of the tyre, with a working load of 80% of the load rating. The vertical stiffness was measured for the different inflation pressures and different tread percentage on the tyre on a flat surface covered with P80 grit sandpaper, a lateral 28x28mm cleat and a longitudinal 28x28mm cleat. The vertical stiffness on a cleat was measured for three cleat positions. The lateral cleat was positioned perpendicular to the direction of travel at 50mm in front of the center line, in-line with the center line and 50mm behind the center line as shown in Figure 4 by the green, red and blue section respectively. The grey shadow indicates the tyre contact patch on a flat surface. Contact between the tyre and the cleat is therefore not distributed over the cleat as a line contact, but instead applied as discrete point loads to the tyre.

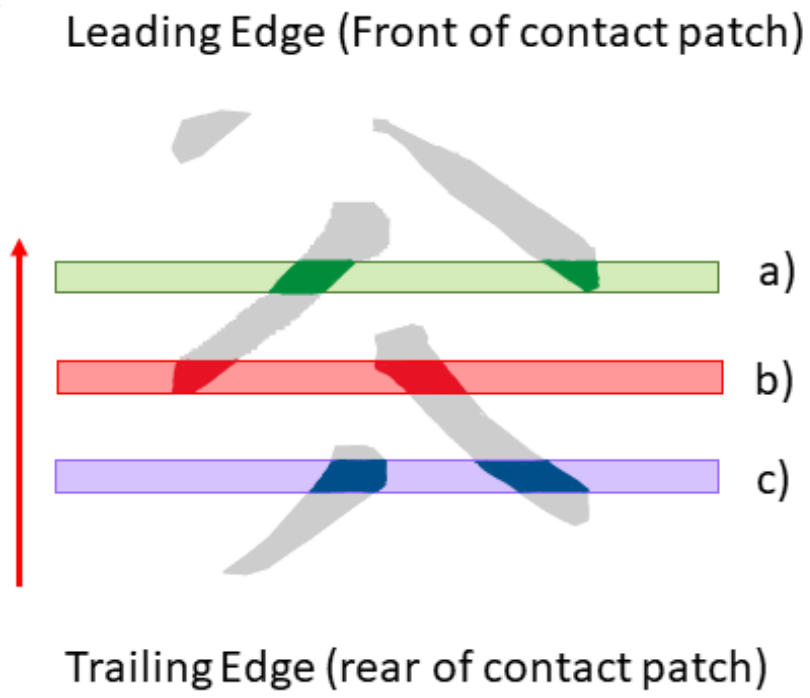

Figure 4: Lateral Cleat positions in contact patch: a) 50mm in front of center, b) in-line with center and c) 50mm behind center.

The longitudinal cleat was positioned in-line with the direction of travel with the cleat 50mm off-set to the inside of the tyre, in-line with the center of the tyre and 50mm off set to the outside of the tyre, as shown in Figure 5 by the green, red and blue sections respectively. These positions were selected to investigate the contribution that the stiffness of the lug in the tread makes to the vertical stiffness of the tyre. These positions had the longitudinal cleat in contact with the center of the lugs (inner and outer cleat position) or the edge of the lugs (in-line with the center of the tyre) as indicated by the darker section for cleat positions a), c) and b), respectively. These points are also the initial contact points about which the tyre deforms up to where the rest of the tyre is in contact with the flat surface below the cleat.

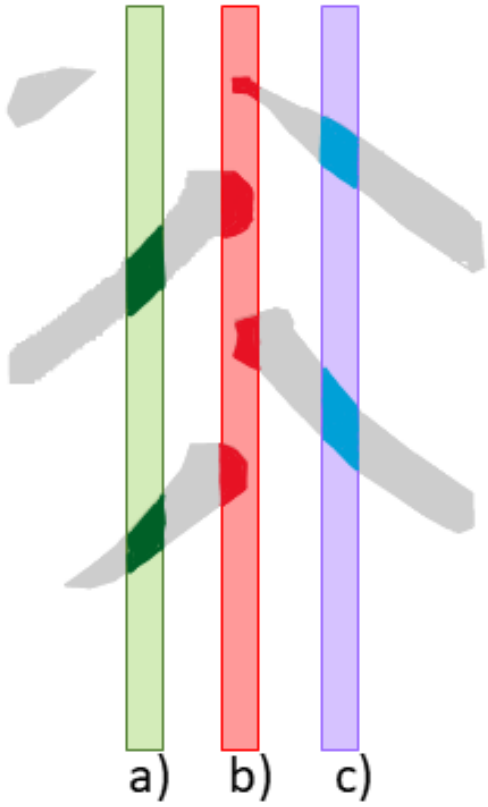

Figure 5: Longitudinal cleat positions in contact patch: a) 50mm off set in, b) in-line with center and c) 50mm off set out.

The lateral and longitudinal stiffness were measured on a flat surface covered with P80 grit sandpaper. The longitudinal stiffness setup on the STTR is shown in Figure 2 with the P80 grit sandpaper surface fitted to the STTR.

4. Results

The results from the tests conducted with different tread wear conditions at 80kPa and 200kPa are discussed in the following sections. In order to maintain the highest integrity of the measurements, the measured data presented was unfiltered during post processing.

4.1 Contact Patch

The size of the tyre contact patch was captured by painting the tyre and applying the 5.68kN vertical load on a white sheet of paper for each inflation pressure and tread wear condition. The footprints for each tread wear condition at 80kPa and 200kPa are shown Figure 6. The red line is a reference indicator of 10mm x 100mm. The thin dashed line shows the change in contact patch perimeter between tread conditions. The contact area was determined by the sum of the black paint print within the perimeter of the footprint.

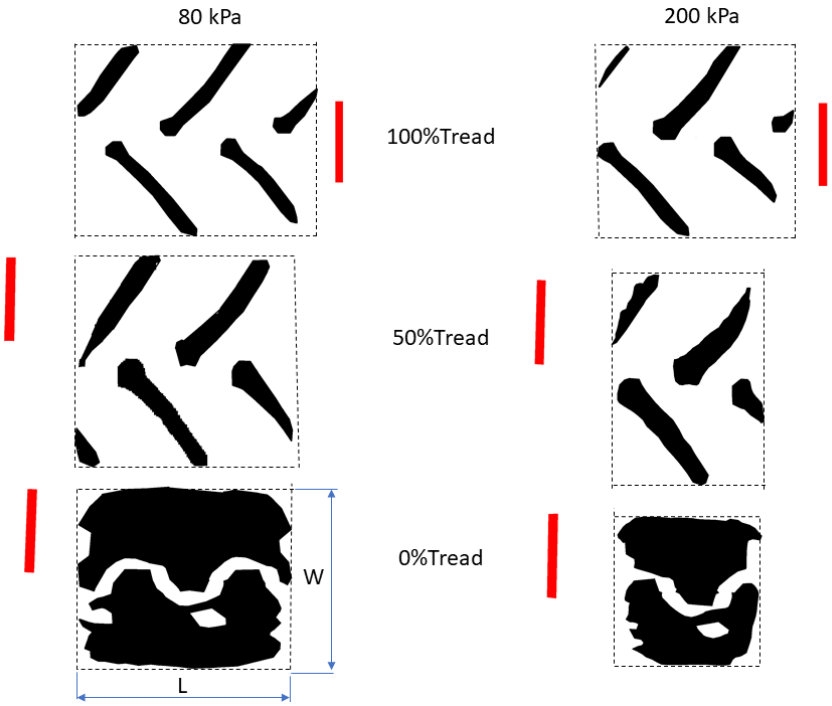

Figure 6: Footprint at different tread conditions and two inflation pressures.

The pressure distribution of the three tread conditions at 200kPa was measured with the use of a TireScan system from Tekscan (2021), connected to an 8001-pressure sensor. The three pressure maps for an inflation pressure of 200kPa are shown in Figure 7.

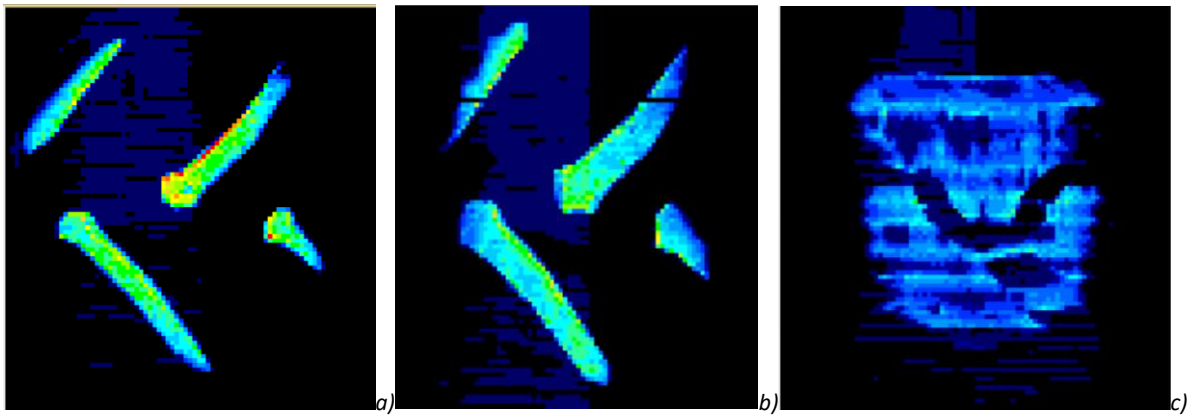

Figure 7: TM700-280/70R16 Pressure distribution at 200kPa for a)100% Tread, b) 50% Tread and c) 0% Tread, respectively.

From the footprints and pressure maps it is noticed that the 100% tread condition has a longer footprint compared to the 50% tread condition which has an overall wider footprint and wider tread blocks. The wider tread blocks are due to the taper shape of the tread block. The 0% tread condition has the smallest perimeter measurements; however, this condition has the highest rubber contact area of the three conditions, thus it has the lowest contact pressure. The contact area, for 0% tread condition and an inflation pressure of 80kPa, increases by 202% compared to the 100% tread condition at 80kPa. The contact area for 0% tread condition for an inflation pressure of 200kPa increases by 147% compared to the 100% tread condition at 200kPa. The change in pressure was estimated with the use of eq. (2).

$$Pressure = \frac{Force}{Area} \qquad \text{eq. (2)}$$

The change in average contact pressure in the footprint due to the change in footprint size/ tread wear condition is presented in Table 2, along with the area of actual rubber in contact area and the perimeter of the contact patch.

Table 2: Estimated change in average contact pressure as a function of tread wear and inflation pressure, with rubber in cantact area and contact perimeter dimentions.

Tread Condition	Constant Vertical Load of 5.68kN					
	200kPa	80kPa	200kPa	80kPa	200kPa	80kPa
	Average Contact Pressure [kPa] from eq. (2)		Rubber in Contact Area [mm^2]		Perimeter of Contact Patch, L x W [mm]	
100% tread	669	476	8490	11909	240x235	300x240
50% Tread	657	492	8642	11534	180x250	265x250
0% Tread	270	157	21021	35993	165x180	265x220

It can be seen in that the contact pressure slightly increases at the lower inflation pressure of 80kPa as the tread wears from 100% to 50%. A 60 to 66% contact pressure drop is noted at 0% tread condition due the increase in actual rubber in contact with the terrain.

4.2 Vertical Static Stiffness on a Flat Surface

The vertical static stiffness was measured on a flat surface using the STTR with P80 grit sandpaper on the flat surface. These measurements are shown in Figure 8. If designers have limited tyre data available they tend to use linear approximations for tyre characteristics. Most tyre models also only account for linear stiffness. The linearized vertical stiffness around the vertical load of 5.68kN, for the tyre in question, is indicated by the dashed blue and dashed green lines for inflation pressures of 200kPa and 80kPa respectively. Figure 8 shows that the characteristics are significantly non-linear and a linear approximation may not be a good approximation when used in ride comfort simulations

over uneven terrain where the vertical load on the tyre can vary between 0 load (wheel losing ground contact) and 4 times the static load (for a 4g axle load). When driving over rough terrain at higher speeds, wheel lift-off occurs regularly and can result in 20% of the time not being in contact with the terrain. On the other extreme when a vehicle becomes air born and lands on one wheel, the vertical wheel load can peak at 4 times the static load. Off-road military vehicles are designed for dynamic loads of between 4 and 5 times the static load. It can be seen that a linear approximation might be adequate when only used for static suspension deformation estimates or driving on smooth terrain. However, should one extrapolate the linear approximation lines (the dashed green and dashed blue lines in Figure 8), with the origin of the lines at zero displacement, a 16% to 21% error can be made in the estimated tyre deformation at the static load. On closer inspection it is clear that the vertical force vs. displacement characteristic is better represented by a parabola rather than a linear line, thus the importance of obtaining accurate tyre data for ride comfort vehicle simulation purposes. It can also be seen that the change in tread condition does not have a large change in gradient of the vertical stiffness between 100% and 50% tread at the static load condition. As the tread nears 0% tread condition the vertical stiffness curve becomes more parabolic and has a larger influence on the vertical stiffness at lower loads. If the vertical load varies by 50% around the static position the vertical stiffness can decrease by up to 30% between 2kN and 3kN and increase by 40% between 9kN and 10kN. This indicates that linearization should always be applied with the use case of the model in mind. Tests were conducted on multiple surfaces which included aluminum, steel, p80 sandpaper and concrete. The tests on different surfaces have indicated that the surface roughness does not affect the vertical stiffness at all.

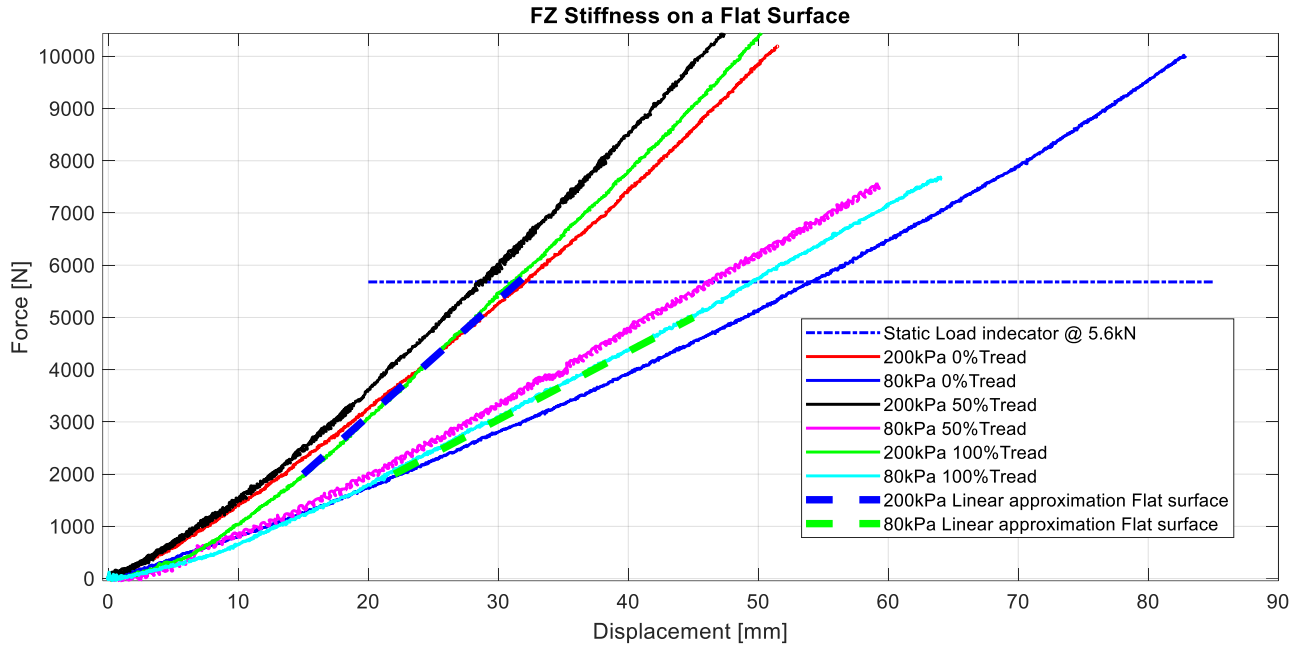

Figure 8: Vertical stiffness measurements for different tread conditions and inflation pressures on P80 grit sandpaper.

4.3 Vertical Static Stiffness on a Lateral Cleat

The effect of the tread wear condition and the position of the lateral cleat has on the vertical stiffness is clearly illustrated in Figure 9. The characteristic of a tyre becomes very non-linear when the tyre travels over a cleat, as shown in Figure 9 for the lateral cleat orientation at 80kPa inflation pressure. Should a linear approximation be made for the vertical stiffness of the tyre one would have to consider a stage 1 stiffness, where the tyre starts to deform over the cleat and a stage 2 stiffness where the tyre comes into contact with the flat surface. Stage 1 can be described as the belt radial stiffness as it is mostly the belt deforming over the cleat. This is also noticed during the first 5 to 10mm vertical deformation on a flat surface where only the belt deforms to start forming the contact patch. Stage 2 can be described as the sidewall radial stiffness which is very dependent on the inflation pressure. On a cleat the transition point to stage 2 will be very dependent on the vertical load during this occurrence as well as the tread wear condition. The location of the transition from stage 1 to stage 2 stiffness over a cleat can change by up to 30mm as the tread wear condition changes, which is the maximum tread

depth on the tyre in question. When comparing the linear approximation of the vertical stiffness on a flat surface, as shown by the dashed lines in Figure 8, with the stage 1 stiffness over a cleat as indicated by the red dashed lines in Figure 9, one can expect a decrease of 45 to 46% in the linear gradient between 80kPa and 200kPa inflation pressure respectively. It can also be seen that the stage 1 stiffness curve, where the tyre is only in contact with the cleat, becomes more convex as the tread wears down.

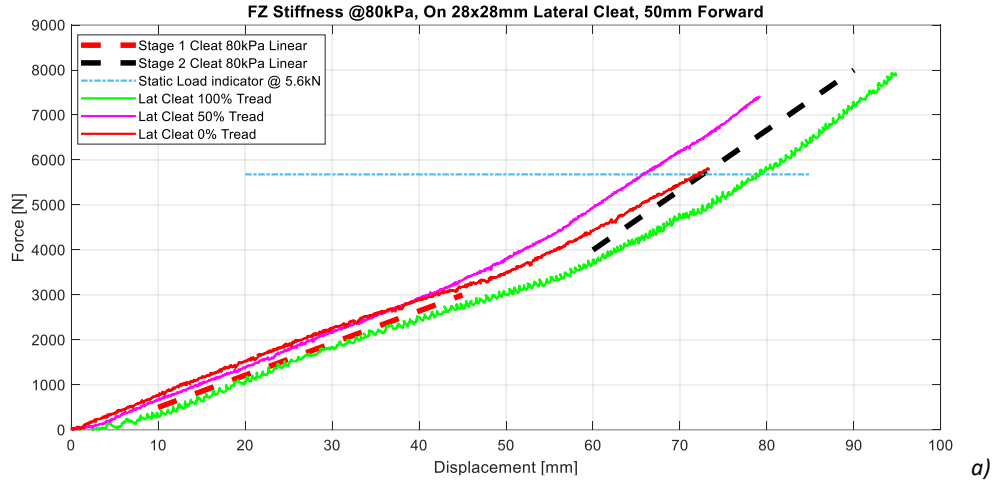

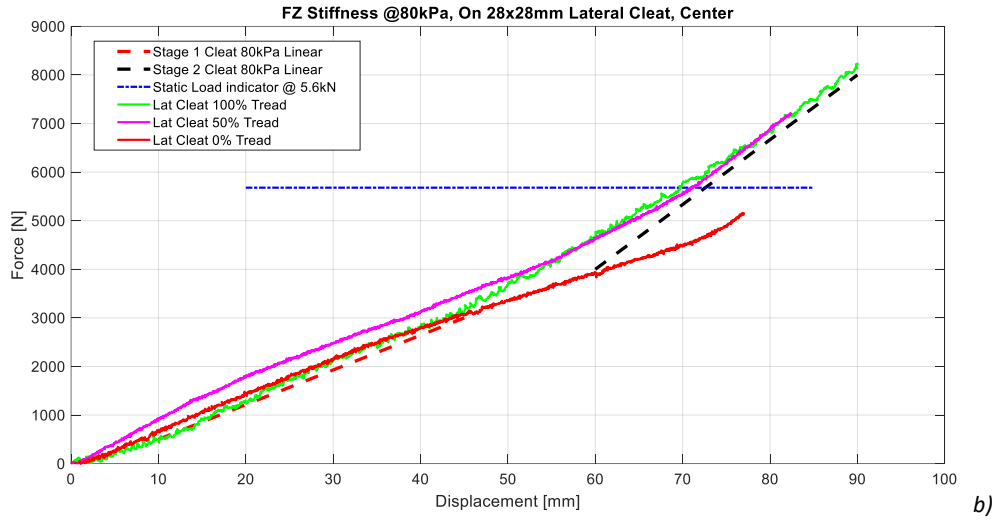

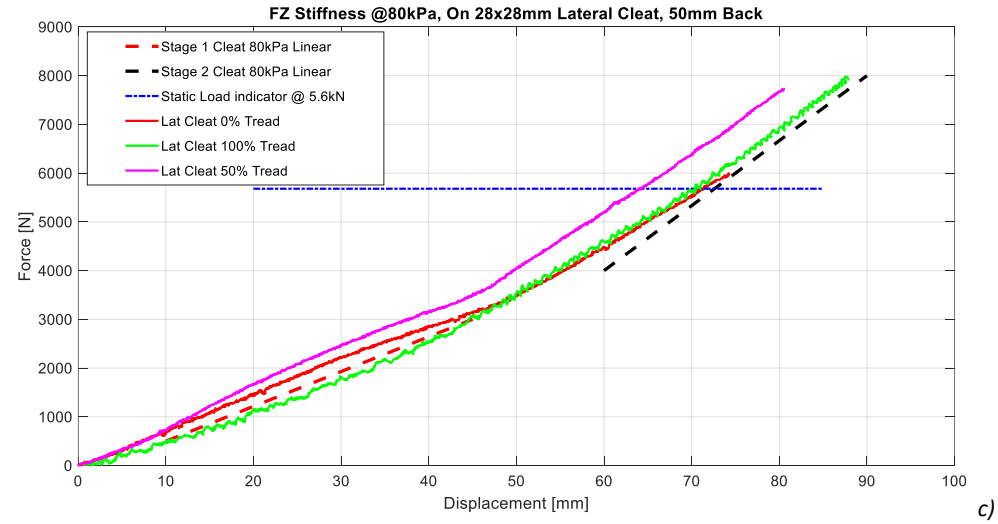

Figure 9: Vertical stiffness on a lateral cleat with different tread conditions for an inflation pressure of 80kPa at a) 50mm forward from the center, b) over the center and c) 50mm back from the center of the wheel, respectively.

This change in linear approximation is illustrated in Figure 10, where all the linear approximations are shown compared to the measurements on a flat surface.

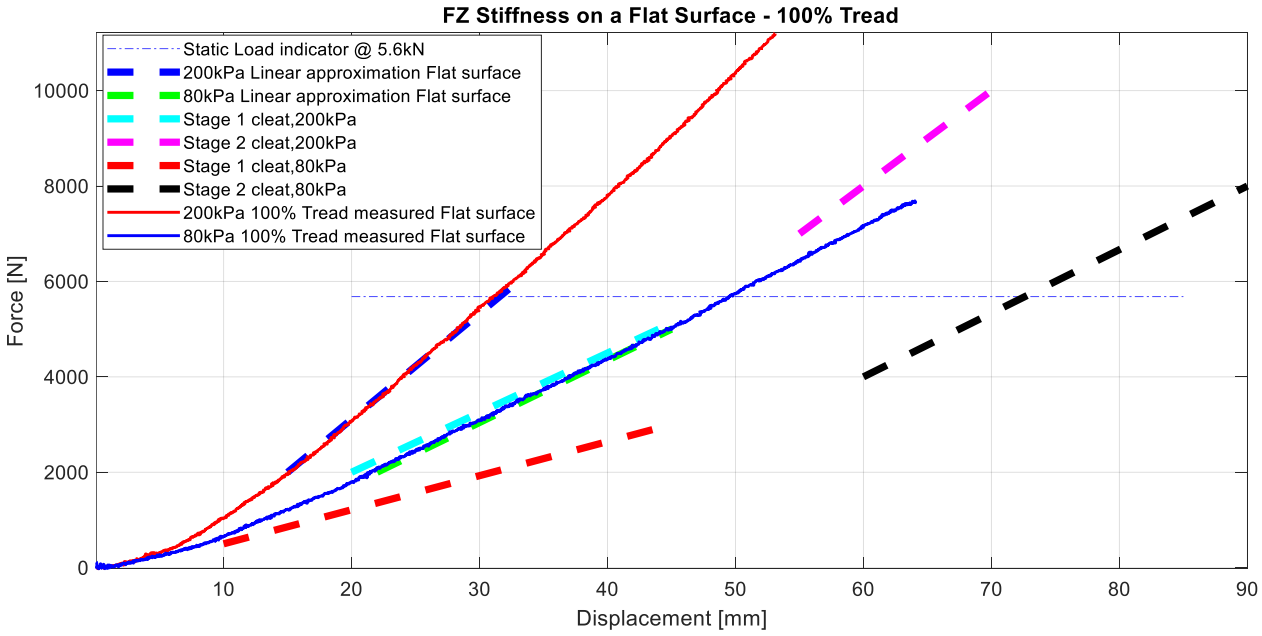

Figure 10: Change in linear approximations for vertical stiffness at 80kPa and 200kPa, with stage 1 and stage 2 over cleats.

The linear stiffness approximations are tabulated in Table 3 and it is clear that a significant change in vertical stiffness occurs when a tyre deforms over a cleat.

Table 3: Linear vertical stiffness approximations.

	Fz Stiffness [N/mm]	Change in Stiffness [%]	% Change relative to
Flat surface contact			
200kPa	222	70	80kPa
80kPa	130		
Cleat contact			
200kPa Stage 1	120	-46	200kPa
200kPa Stage 2	200	-10	200kPa
200kPa Stage 1	71	-45	80kPa
200kPa Stage 2	133	2	80kPa

4.4 Vertical Static Stiffness on a Longitudinal Cleat

The change in vertical stiffness due to different inflation pressures, 80kPa and 200kPa, with different tread wear conditions for a longitudinal cleat in the center of the wheel is shown in Figure 11a) and Figure 11b), respectively. To illustrate the difference between lateral and longitudinal cleats the same stage 1 and stage 2 linear approximations are added to the graphs in Figure 11. It is shown that the vertical stiffness characteristic of the tyre does not change as much for different lateral positions of the longitudinal cleat when compared to the effect different tread wear conditions have at the center of the wheel.

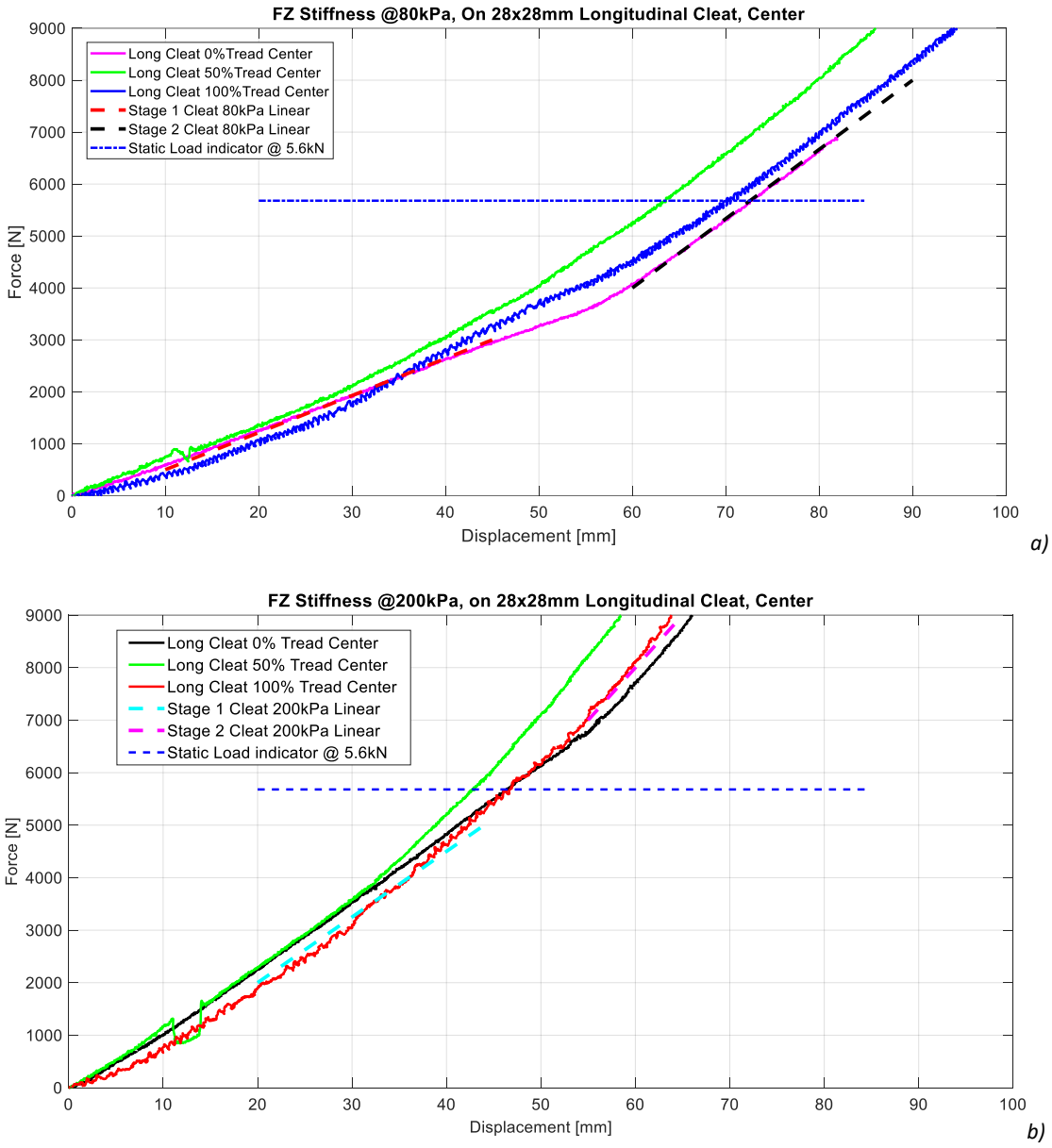

Figure 11: Vertical stiffness change due to a longitudinal cleat at different tread wear conditions, at 80kPa and 200kPa respectively.

Figure 12 is a very good representation of how the tyre will react over different cleat orientations for different tread wear conditions. The stage 1 and stage 2 linear stiffness approximations as described above are also shown in Figure 12a), it can be seen that of the same inflation pressure at 100% tread condition the tyre stiffness is relatively small (in the order of 10% difference) for a lateral or longitudinal oriented cleat. This changes significantly as the tyre tread wear condition changes from 100% to 0% tread. Figure 12b) and Figure 12c) respectively, show that the stiffness transition point

from stage 1 to stage 2 moves and requires more vertical displacement to take place with less tread on the tyre.

The figures in this section show that when a tyre travels over a cleat in the lateral or longitudinal orientation, one can expect up to a 46% decrease in vertical stiffness with up to a 10% change in stiffness during stage 2, depending on the tread wear condition, where the vertical stiffness returns to nearly the same stiffness as measured on a flat surface at high vertical loads. The combined tread block and belt radial stiffness contribute to lower vertical stiffness at lower vertical loads whereas at higher vertical loads the main contribution to the vertical stiffness is from the compression of the air volume inside the tyre which translates to the side wall radial stiffness. It is noted that the transition from stage 1 to stage 2 stiffness is tread wear dependent and independent of the inflation pressure as indicated by the green dash lines in Figure 12 for the lateral cleat and the green dash-dot lines for the longitudinal cleat.

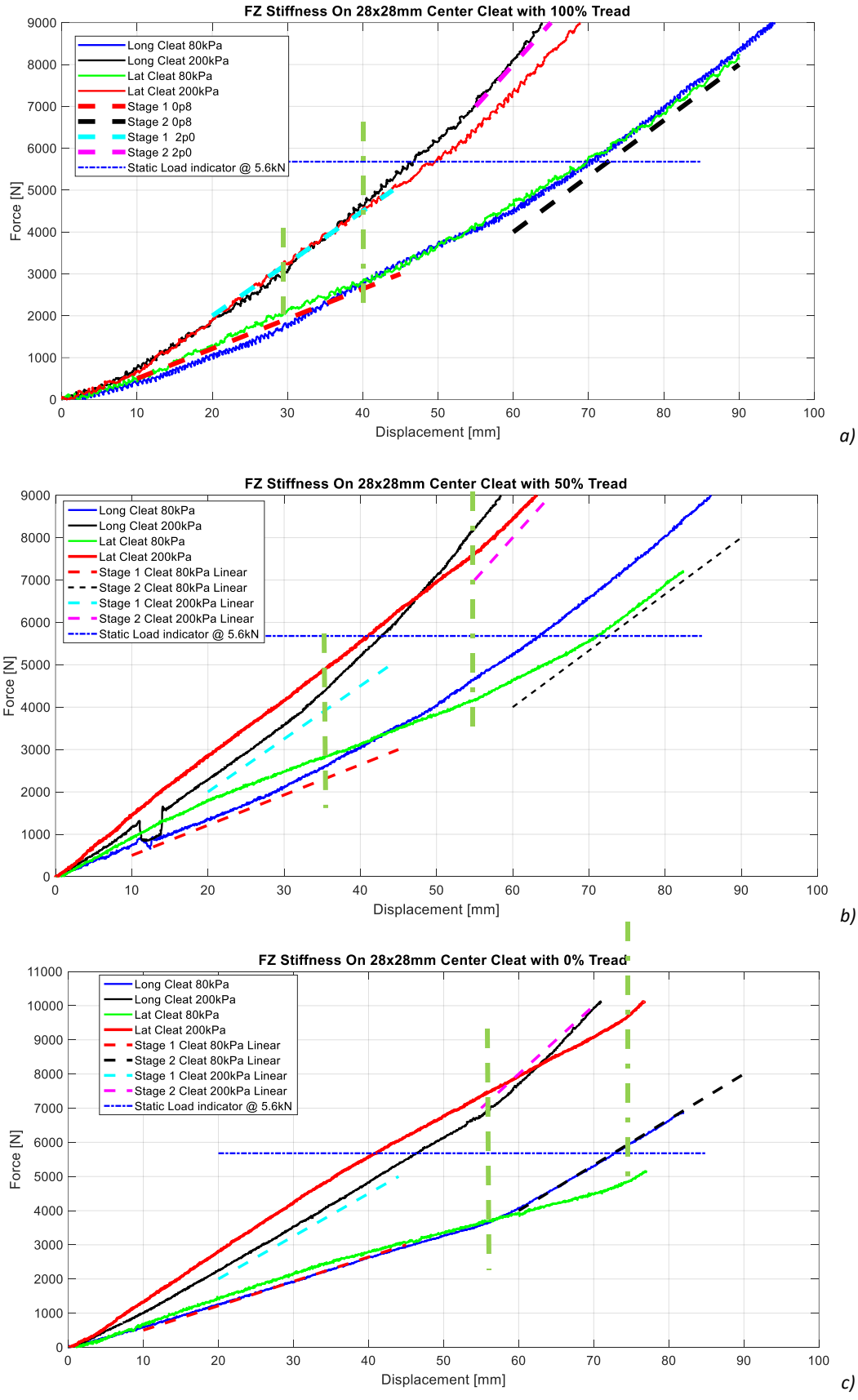

Figure 12: Vertical stiffness comparison over lateral and longitudinal cleats at 80kPa and 200kPa for different tread wear conditions.

The stiffness transition from stage 1 to stage 2 can be estimated by calculating the beam deflection of a simply supported beam, as described in eq 3 (Shigley, 1986), for a single point contact at the center of the beam. The beam in this case is the lug and carcass of the tyre deforming about the cleat as shown in Figure 13.The assumption of a single point contact is made due to the size of the cleat, in the order of 10 to 20% relative to the dimensions of the contact patch and length of the lug/beam. The point contact approximation also eliminates the effect of the cleat-lug cross interaction which is in the order of 45 degrees for a lateral or longitudinal oriented cleat as shown in Figure 4 and Figure 5, respectively.

$$\delta_{lugFz} = \frac{F_z \, {l_{lug}}^3}{48 \, E \, I_{tread}} \qquad \text{eq (3)}$$

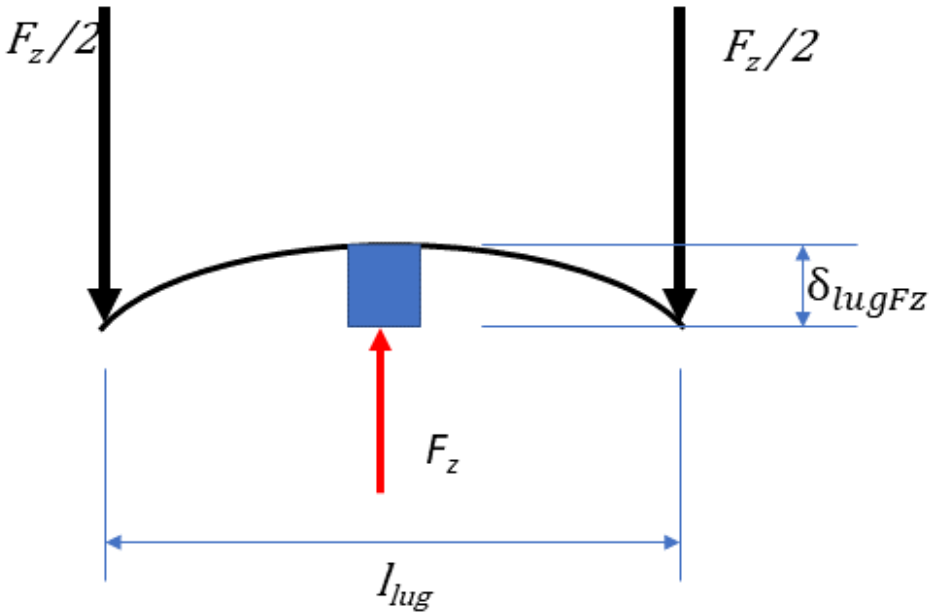

Figure 13: Deflection of lug around a cleat.

The applied force, F_z, is determined from measured results with 100% tread condition, where F_z is adjusted until the same deflection is calculated at the transition point, 30mm and 40mm as indicated by the green dash and dash-dot lines in Figure 12a) for the longitudinal and lateral cleat orientation,

respectively. The same force can then be used to estimate the deflection for different tread wear conditions. The force values used were $F_{static}/4$ and $F_{static}/3$ for the longitudinal and lateral cleats respectively. The length of the lug, l_{lug}, as measured on the tyre, is 165mm for the tyre in question. The Young's modulus for the rubber, *E*, was calculated with the use of eq 4 (cosin scientific software, 2017), with the use of the measured Shore A Hardness value, s, of 65 for the tyre in question.

$$E = 218300(1.0482792^{s}) \qquad \text{eq (4)}$$

The moment of inertia of the lug section, I_{tread}, is determined from the cross section of the lug and thickness of the carcass of the tyre as shown in Figure 14, with the base width the distance between 2 lugs on the tyre, which is 108mm for the tyre in question.

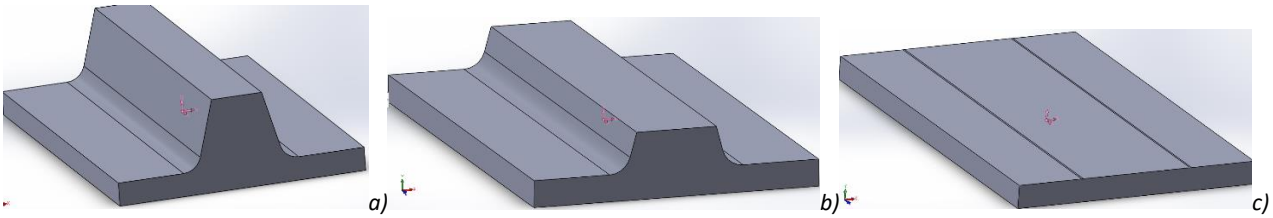

Figure 14: Cross section for a)100% Tread, b)50% tread and c)0% tread.

The results from the calculated and measured deflection, as indicated by the green dash and dash-dot lines in Figure 12, is tabulated in Table 4. When comparing the calculated deflection to the measured deflection the maximum error is in the order of 8.5%. This analysis indicates the direct relationship between the tyre stiffness over the cleat and the lug geometry, which is seen to be independent of the tyre inflation pressure.

Table 4: Stage 1 to Stage 2 transition point, measured vs. calculated

		Tread Condition		
	Cleat orientation	**100%**	**50%**	**0%**
Measured Deformation[mm]	Lateral	40	55	75
	Longitudinal	30	36	55
Calculated Deformation[mm]	Lateral	40.5	52.1	78.6
	Longitudinal	30.4	39.0	59.0
	% Difference from measured	**-1.2**	**5.3**	**-4.8**
		-1.2	**-8.5**	**-7.2**

4.5 Longitudinal Static Stiffness Measurement Results

The longitudinal static/non-rolling stiffness measurements were conducted on the STTR on P80 grit sandpaper as shown in Figure 2. This directional characteristic can also be referred to as the tangential stiffness. Similar longitudinal stiffness is measured in the linear section between -40mm and 40mm longitudinal displacement of 100% to 50% tread condition at an inflation pressure of 80kPa and 200kPa. The longitudinal stiffness and maximum traction force increase significantly as the tread wear condition nears 0% as shown in Figure 15.

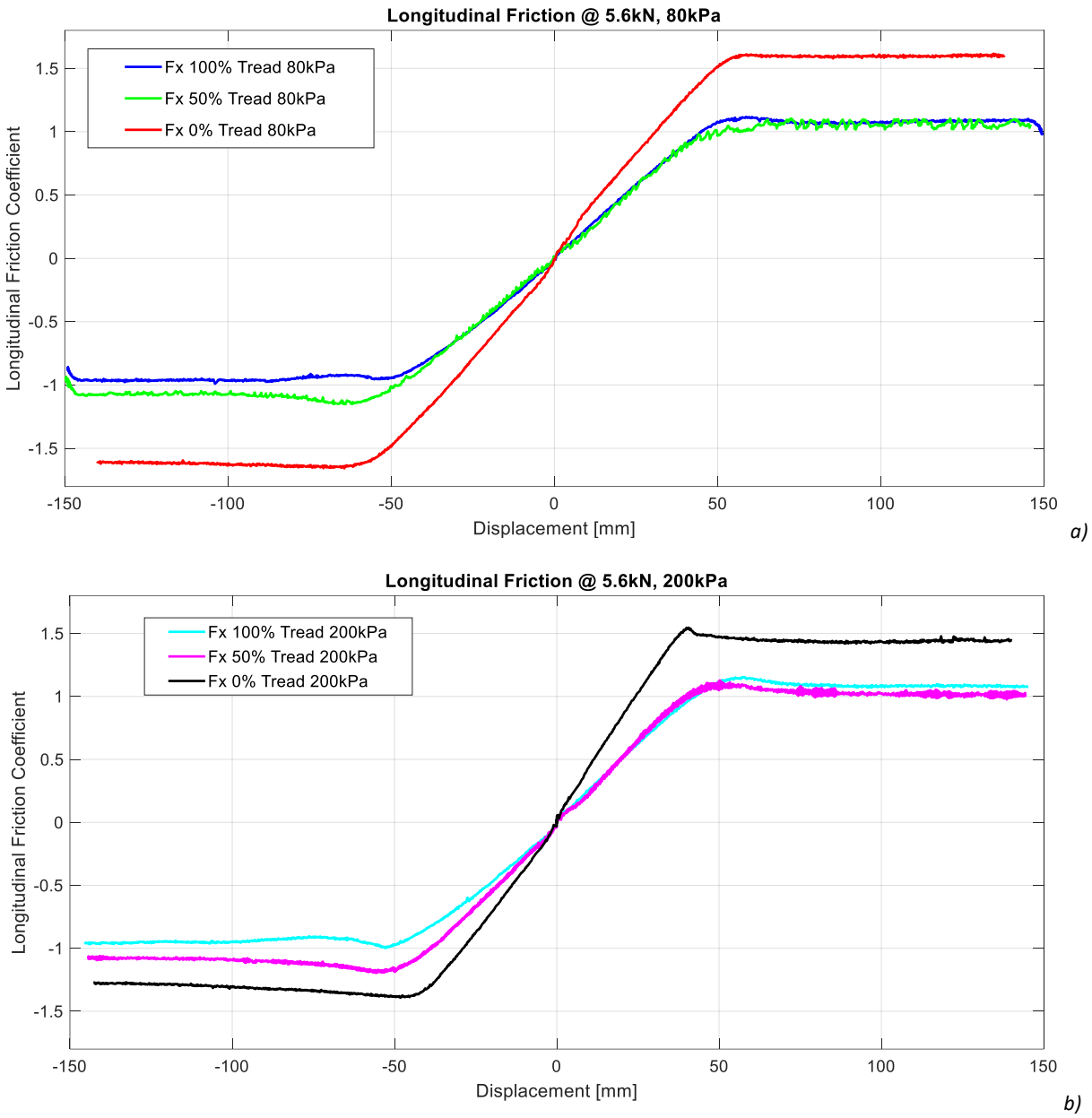

Figure 15: Longitudinal stiffness measurements for inflation pressure of a)80kPa and b)200kPa, respectively for different tread wear conditions.

The increase in maximum traction force at 0% tread condition is directly related to the dramatic increase of rubber in contact with the surface in the contact area as shown in Figure 6. At 0% tread the sidewall tangential stiffness is measured and is directly proportional to the inflation pressure as shown in Figure 15. At 200kPa inflation pressure the effect of the lugs in the tread deforming

differently for positive and negative displacements are noted in Figure 15b). This indicates that the tread stiffness varies for opposite deformation. At 0% tread condition the tyre carcass is the only component contributing to the longitudinal stiffness of the tyre, compared to the 50% and 100% tread condition where the lugs in the tread supply additional stiffness to the system. The tyre carcass and lugs can thus be simplified to two springs in series, where the spring with the lowest stiffness will deform/displace the most. This indicates that the tread has a lower stiffness compared to the tyre carcass. It is found that the change in longitudinal stiffness in the linear region for different tread wear conditions and inflation pressures can increase by up to 24% with a thread wear change from 100% tread to 50% tread and an increase of up to 63% between 100% tread and 0% tread condition. The change in longitudinal stiffness can be a function of the carcass construction depending if the tyre is used as a driven or non-driven wheel. The lateral deformation of the lugs in the contact patch can also contribute to the longitudinal stiffness, where the lugs are compressed together or pulled apart during opposite longitudinal displacement as shown in Figure 16.

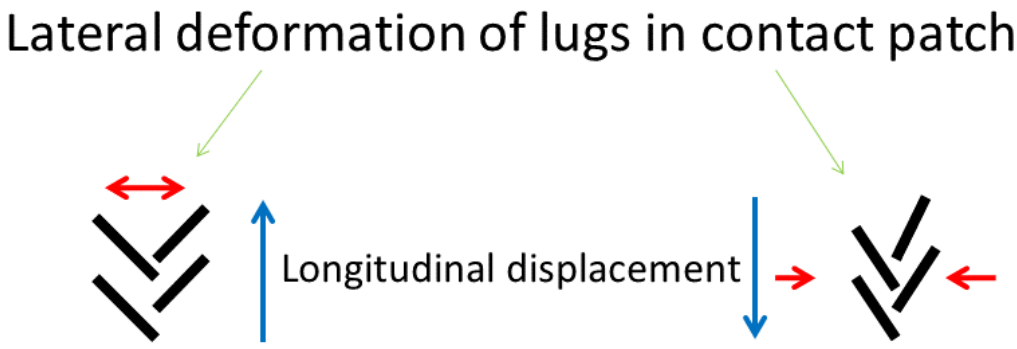

Figure 16: Lateral lug deformation in contact patch during longitudinal displacement.

The bending of the lugs during the longitudinal displacement for a tyre with 50% tread depth at 200kPa is shown in Figure 17. In this figure the tyre on the right represents a tyre with only vertical deformation present. The tyre on the left is displaced by 150mm in the longitudinal direction to the

left. It can be seen how the sidewall deforms in a tangential direction during the 150mm longitudinal deformation, this is shown by the red lines relative to the white markings on the tyre sidewall in Figure 17. The yellow line in Figure 17 represents the orientation of the top of the tread block before any longitudinal deformation. The green line in Figure 17 shows how much the tread block deforms due to the bending moment generated as described previously.

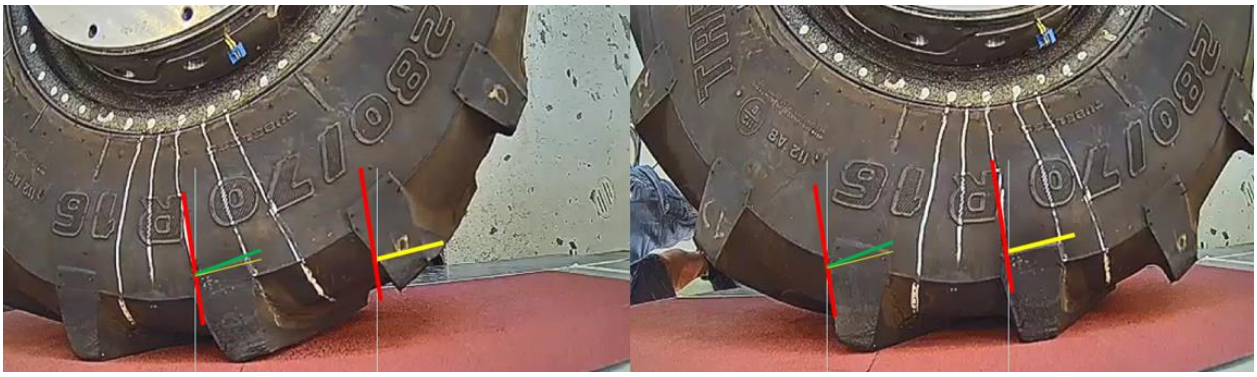

Figure 17: Tread deformation at 150mm and 0mm longitudinal deflection, respectively at 50% tread and 200kPa inflation pressure.

The bending of the lugs during the longitudinal displacement for a tyre with 100%, 50% and 0% tread depth, respectively, at 200kPa is shown in Figure 18. It can be seen that the sidewall tangential stiffness remains constant and is independent of the tread depth. This is shown by the red line in Figure 18 which remains in-line with the white markings on the tyre sidewall, irrespective of the amount of tread on the belt. The green line in Figure 18 shows how much the tread block deforms due to the bending moment generated as described previously. This deformation is the same for 100% tread and 50% tread. The yellow line in Figure 18 again represents the orientation at the top of the tread block before any longitudinal deformation, it can be seen that no deformation is noted at this position when the tread blocks have been removed from the tyre.

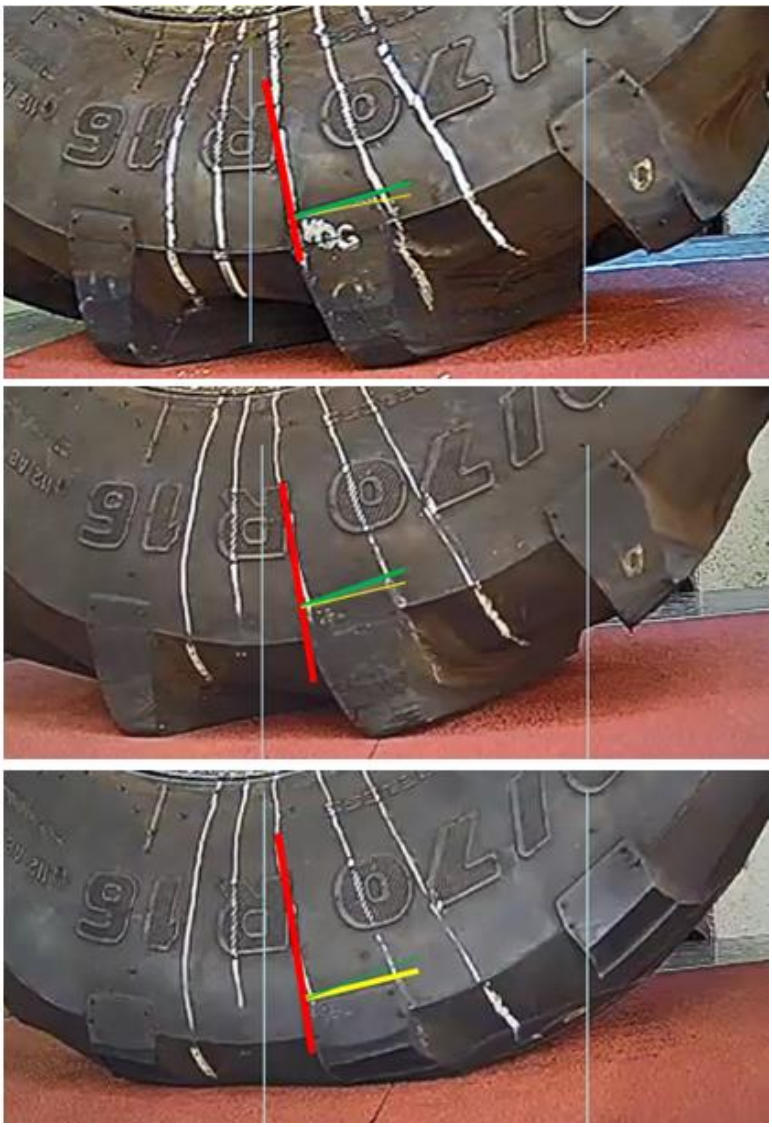

Figure 18: Longitudinal lug and carcass deformation at 200kPa inflation pressure for 100% tread, 50% tread and 0% tread, respectively.

The graphic representation that the sidewall tangential stiffness is directly dependent on the inflation pressure is shown in Figure 19. The red lines in Figure 19 have the same inclination as the red lines in Figure 17 and Figure 18 for the tyre at an inflation pressure of 200kPa. When comparing the red line on the left tyre in Figure 19 to the white markings in the tyre one can see the change in the sidewall tangential stiffness as the inflation pressure is decreased to 80kPa.

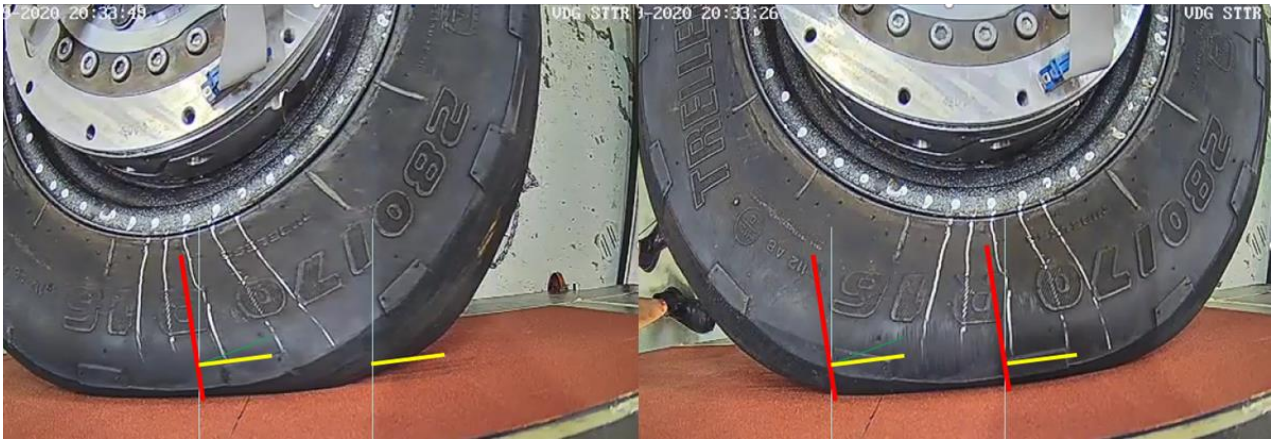

Figure 19: Sidewall tangential stiffness change at 150mm and 0mm longitudinal deflection, respectively at 0% tread and 80kPa inflation pressure.

4.6 Lateral Static Stiffness Measurement Results

The lateral static/non-rolling stiffness measurements were conducted on the STTR on P80 grit sandpaper. Similar lateral stiffness is measured in the linear section between -50mm and 50mm lateral displacement for 100% to 50% tread condition at an inflation pressure of 80kPa. The lateral stiffness and maximum friction coefficient increase as the tread wear condition nears 0% as shown in Figure 20.

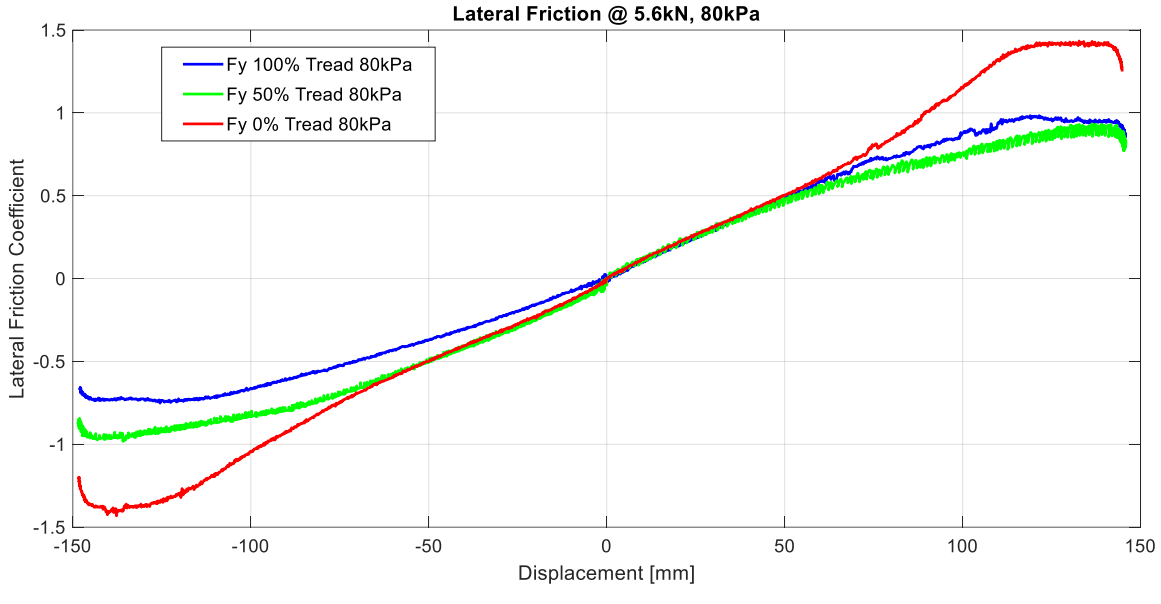

a)

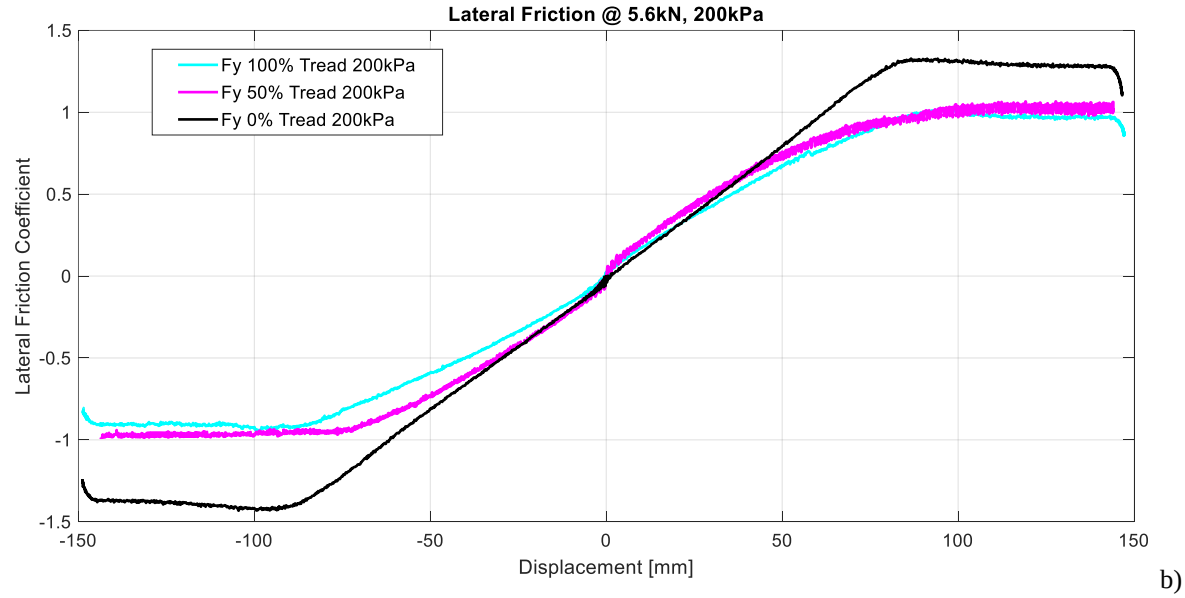

b)

Figure 20: Lateral stiffness measurements for inflation pressure of a) 80kPa and b)200kPa, respectively for different tread wear conditions.

An increase in maximum lateral force at 0% tread condition is again directly related to the dramatic increase of rubber in contact with the surface in the contact area as shown in Figure 6. At 200kPa inflation pressure the effect of the lugs in the tread deforming differently for positive and negative displacements are noted in Figure 20b). This indicates that the tread stiffness varies for opposite

lateral displacement and is dependent on the position of the lugs in the contact patch as an un-symmetrical lug distribution is always present in the contact patch as seen in Figure 6. At 0% tread condition the tyre carcass is the only component contributing to the lateral stiffness of the tyre, thus a symmetrical characteristic is measured, compared to the 50% and 100% tread condition where the lugs in the tread supply additional stiffness to the system. This will continuously change as the lugs move through the contact patch, as a result an oscillating lateral force is always present during measurements on a rolling tyre. The most efficient way to eliminate this occurrence is to inflate the tyre at the required static load until equal amounts of lugs are in the contact patch. The tyre carcass and lugs can again be simplified to two springs in series, where the spring with the lowest stiffness will deform/displace the most and as a result lowers the lateral stiffness. It is noted that the tread's stiffness increases as the tread wear condition lowers from 100% tread to 50% tread. It is found that the change in lateral stiffness (from -50 to 50mm displacement) in the linear region for different tread wear conditions and inflation pressures can increase up to 29 % with a thread wear change from 100% tread to 50% tread and an increase of up to 51% between 100% tread and 0% tread condition at an inflation pressure of 200kPa. The same correlation is seen in the maximum sliding friction coefficient (at -120mm and 120mm displacement) as the tread wear conditions changes. The drastic change in grip at 0% tread can change the characteristic of a vehicle which tends to slide/under steer in an emergency evasive maneuver, such as a lane change, to a vehicle that may roll-over during the same maneuver. As agricultural vehicles tend to have high centers of gravity and are prone to roll-over, the change in lateral grip is a very important aspect to take note of during tyre wear.

5. Conclusion

This study has shown the importance of understanding the effect the condition of tyres will have on the response one can expect from a vehicle. This is especially the case on the majority of agricultural

vehicles where the tyre is the suspension of the vehicle. The vertical stiffness measurements have shown that the change in tread condition does not have a drastic change in gradient of the vertical stiffness between 100% and 50% tread around the static load condition, however as the tread nears 0% tread condition the vertical force vs. displacement curve becomes more parabolic. When extrapolating the linear stiffness around the static vertical load, a 16% to 21% error can be made in the estimated tyre deformation. As a tyre travels over a cleat one can expect a 46% decrease in vertical stiffness which leads to a multistage stiffness graph where the vertical stiffness increases again to the stiffness of a tyre on a flat surface as the tyre deforms around the cleat. At 100% tread condition the tyre vertical stiffness is relatively similar over lateral and longitudinal cleats, however this changes as the tread wear condition changes. It is noted that the transition point, form a lower to a higher stiffness, on the vertical force vs. displacement graph, is dependent on the tread wear condition and independent of the inflation pressure. It is found that the transition point can be calculated within 8.5% with the use of simply supported beam deflection theory and the cross section geometry of the lug at different tread wear conditions.

It is found that the change in longitudinal stiffness in the linear region for different tread wear conditions and inflation pressures can increase up to 24 % with a thread wear change from 100% tread to 50% tread. Longitudinal stiffness increases of up to 63% between 100% tread and 0% tread condition at an inflation pressure of 80kPa is measured. The dramatic increase in friction coefficient in the longitudinal direction, at 0% tread, can place high levels of unintended strain on the driveline of the vehicle which may lead to driveline failures.

The change in lateral stiffness in the linear region for different tread wear conditions and inflation pressures can increase by up to 29 % with a thread wear change from 100% tread to 50% tread. A lateral stiffness increase of up to 51% between 100% tread and 0% tread condition at an inflation pressure of 200kPa is measured. This drastic change in grip at 0% tread can change the characteristics

of a vehicle which tends to slide/under steer in an emergency evasive maneuver, such as a lane change, to a vehicle that may roll over during the same maneuver. It is recommended that each tyre model used in a simulation environment is parameterized with representative tyre data so that the non-linearities are captured in the tyre model.

It is suggested that physics based tyre models (example, FTire) is first parameterized with tyre data for a tyre with 0% tread. This data should be used to parameterize mainly the carcass parameters, followed by adding the parameters for the brush/contact model with the use of the data gathered from a tyre with 100% tread.

This study also shows the importance of knowing the difference in traction due to tyre wear and why actual tyre data may assist designers with improved simulation results for ride and handling simulations. Although it is the responsibility of the end user to maintain the tyres on the vehicle, it remains the OEM's responsibility to design a vehicle that can function reliably for different tyre wear conditions. It is also shown that running tyres at the correct inflation pressure, for the specific vertical load that the tyre is operating at, has a direct impact on the tyre's response. The standard procedure of testing a tyre only in the "new" condition and using only this data to parameterize the tyre model can lead to substantial errors in the design process of a vehicle. Future studies should be conducted to investigate the effect of scaling on larger agricultural tyres as well as the effect of the friction coefficient provided by different contact surfaces.

References

Ambruster, K., and Kutzbach, H.D., 1989. Development of a single wheel tester for measurement on driven angled wheel. In: Proceedings of 5th European conference of the ISTVS, Wageningen, The Netherlands; p. 8–14.

Becker, C.M. and Els, P.S., 2018, Static and Dynamic Parameterization Test Rigs for Large Tyres, Proceedings of the 10th Asia-Pacific Conference of the ISTVS, Kyoto, Japan, July 11-13.

Becker, C.M. and Els, P.S., 2020, Motion Resistance Measurements on Large Lug Tyres, Journal of Terramechanics, Vol.88(1), p.17-27.

Billington, P.W., 1973 The NIAE Mk II single wheel tester. J Agric Eng Res ;18:67–70.

Cosin scientific software, 2017, FTire, Modelization and Parameter Specification. 2017-1-r14630. [pdf]. Software documentation and user guide.

Crolla, D.A. and El-Razaz, A.S.A., 1987, A Review of The Combined Lateral and Longitudinal Force Generation of Tyre on Deformable Surfaces. Journal of Terramechanics, Vol. 24(3), p199-225.

Crolla, D.A., and Maclaurin, E.B., 1985, Theoretical and Practical Aspects of The Ride Vibration Dynamics of Off-road Vehicles., Journal of Terramechanics, Vol 22(1), p17-25.

Dressler, K., Speckert, M. and Bitsch, G., 2009, Virtual durability test rigs for automotive engineering, Vehicle System Dynamics, 47:4, 387-401, DOI: 10.1080/00423110802056255

fka, 2021. Chassis Truck Tyre Test Rig, Aachen, Germany, https://www.fka.de/en/testing/chassis/114-truck-tyre-test-rig.html, assessed on 26 March 2021.

Karafiath, L.L. and Nowatzki, E.A., (1978). Soil Mechanics for Off-Road Vehicle Engineering (1st ed.). Germany: Trans Tech Publications.

Lines, J.A., 1991, The Suspension Characteristics of Agricultural Tractor Tyres. PhD thesis, Cranfield Institute of Technologu Silsoe College.

Mardani, A., Shahidi, K. and Maslak H. K., 2010, An Indoor Traction Measurement System to Facilitate Research on Agricultural Tires. Journal of Food, Agriculture and Environment, Vol. 8(1), p.642-646.

Misiewicz, P.A., 2010. The Evaluation of the Soil Pressure Distribution and Carcass Stiffness Resulting From Pheumatic Agricultural Tyres. (PhD. Thesis) Cranfield, UK: Cranfield University.

Misiewicz, P.A., Terence, E.R., Blackburn, K., Godwin, R., 2016, Comparison of Methods for Estimating the Carcass Stiffness of Agricultural Tyre on Hard Surfaces, Biosystems Engineering, Vol 147, pp 183-192.

MTS,2021. Flat-Trac Tire Force & Moment Measurement Systems, MN USA https://test.mts.com/en/products/automotive/tire-test-systems/flat-trac-tire-system#technical, accessed on 26 March 2021.

Murphy, K. and Lines, J.A., 1991.The Stiffness of Agricultural Tractor Tyres. Journal of Terramechanics, Vol. 28(1), pp49-64.

Shigley, J.E., 1986, Mechanical Engineering Design, First Metric Edition, Appendix Tables A-9, #5 Simple supports-center load.

Shmuleviuch, I., Ronai, D., Wolf, D., 1996. A new field single wheel tester. Journal of Terramechanics, Vol. 33(3), p133–41.

Stayner, R.M., Collins, J.A. and Lines, J.A., 1984, Tractor Ride Vibration Simulation as an Aid to Design. Journal of Agricultur Engineering Res. 29.345-355.

Tekscan, 2021. Tekscan Pressure Mapping, Force Measurement and Tactile Sensors, South Boston, MA, USA: https://www.tekscan.com/products-solutions/systems/tirescan-versatek-system, accessed on 9 April 2021.

Witzel, P., 2018. The Hohenheim Tyre Model: a Validated Approach For The Simulation of High Volume Tyres – Part I: Model Structure and Parameterisation. J. Terrramech, Vol. 75, p3–14.

Wright, K.R.S., Botha, T.R. & Els, P.S. 2019, 'Effects of age and wear on the stiffness and friction properties of an SUV tyre', Journal of Terramechanics, vol. 84, pp. 21-30.